Journal of Theoretical Biology 430 (2017) 221–228

Contents lists available at ScienceDirect

Journal of Theoretical Biology

journal homepage: www.elsevier.com/locate/jtbi

A note on stress-driven anisotropic diffusion and its role in active deformable media

Christian Cherubini[a,b], Simonetta Filippi[a,b], Alessio Gizzi[a], Ricardo Ruiz-Baier[c,*]

[a] Unit of Nonlinear Physics and Mathematical Modeling, Department of Engineering, University Campus Bio-Medico of Rome, Via A. del Portillo 21, 00128 Rome, Italy

[b] International Center for Relativistic Astrophysics, I.C.R.A., University Campus Bio-Medico of Rome, Via A. del Portillo 21, 00128 Rome, Italy

[c] Mathematical Institute, University of Oxford, A. Wiles Building, Radcliffe Observatory Quarter, Woodstock Road, Oxford OX2 6GG, United Kingdom

ARTICLE INFO

Article history:
Received 11 May 2017
Revised 10 July 2017
Accepted 13 July 2017
Available online 26 July 2017

Keywords:
Active deformable media
Stress-assisted diffusion
Reaction-Diffusion
Electro-Mechanics
Finite elasticity
Cardiac dynamics

ABSTRACT

We introduce a new model to describe diffusion processes within active deformable media. Our general theoretical framework is based on physical and mathematical considerations, and it suggests to employ diffusion tensors directly influenced by the coupling with mechanical stress. The proposed generalised reaction-diffusion-mechanics model reveals that initially isotropic and homogeneous diffusion tensors turn into inhomogeneous and anisotropic quantities due to the intrinsic structure of the nonlinear coupling. We study the physical properties leading to these effects, and investigate mathematical conditions for its occurrence. Together, the mathematical model and the numerical results obtained using a mixed-primal finite element method, clearly support relevant consequences of stress-driven diffusion into anisotropy patterns, drifting, and conduction velocity of the resulting excitation waves. Our findings also indicate the applicability of this novel approach in the description of mechano-electric feedback in actively deforming bio-materials such as the cardiac tissue.

1. Introduction

Excitable media, whether of biological type or not, represent complex nonlinear systems which are often of electrochemical nature, and can typically be coupled to several multi-physical factors as heat transfer or solid and/or fluid mechanics. A remarkable example is the heart, where nonlinear bioelectrical waves propagate on a complex anatomical medium undergoing large mechanical deformations and facing strong interactions with biological fluids. More precisely, cardiac contraction results from the combination of a complex emerging behaviour where subcellular ion dynamics induce the overlapping of protein filaments, rapidly scaling up to both the cellular and tissue scales through a process known as excitation-contraction coupling and, as main topic of the present work, its reverse effect known as the *mechano-electric feedback* (MEF) (Kaufmann and Theophile, 1967; Kohl and Sachs, 2001). Studying the spatiotemporal dynamics of excitation waves in the heart is of paramount importance in the understanding of a large class of processes including depolarisation, repolarisation and period doubling bifurcations occurring in the transition towards chaotic regimes (arrhythmias) (Chen et al., 2017; Das et al., 2014; Tran et al., 2009).

Still in the context of cardiac dynamics, a large number of experimental data is available to describe ionic and electrophysiological processes at many spatio-temporal scales. However, due to diverse technical reasons, a common practice is to biochemically suppress any mechanical feedback to record these data, implying that any back-reacting effect intrinsically due to electromechanical interactions is systematically neglected. Nevertheless, the importance of understanding the interplay between the reaction-diffusion (RD) dynamics with mechanical deformation is quite clear, and a recent growing interest in refining a companion mathematical model for the dynamics of higher complexity models has been observed (Quinn, 2014; 2015; Quinn et al., 2014; Ravelli, 2003). Even though several subcellular contributors to cardiac MEF have been extensively studied (as for instance, stretch-activated ion channels (Ward et al., 2008)), their proper and consistent integration into tissue-level models has remained a challenging task; further having a very limited clinically-translatable application and validation.

In the last fifteen years, the relation between cell or tissue-based electrophysiology models with mechanical deformation of soft tissues has been formulated in terms of active stress (Nash and Panfilov, 2004), active strain (Cherubini et al., 2008;

* Corresponding author.
E-mail addresses: c.cherubini@unicampus.it (C. Cherubini), s.filippi@unicampus.it (S. Filippi), a.gizzi@unicampus.it (A. Gizzi), ruizbaier@maths.ox.ac.uk (R. Ruiz-Baier).

http://dx.doi.org/10.1016/j.jtbi.2017.07.013
0022-5193/

Gizzi et al., 2015; Nobile et al., 2012), with the addition of stretch-activated currents (Panfilov and Keldermann, 2005; Panfilov et al., 2007; Quinn and Kohl, 2013; Trayanova et al., 2011), or recently combined with either membrane capacitance changes (De Oliveira et al., 2015), or with inertial effects (SahliCostabal et al., 2017). However, in all of these works the key physical ingredient ruling the spatio-temporal dynamics of the membrane potential, i.e. the diffusion (in this context, the conductivity tensor), has been commonly considered independent of mechanical deformation when related with the current configuration of the body. Even if general constitutive prescriptions suggesting a possible interaction were advanced (Nash and Panfilov, 2004), the resulting MEF coupling due to the pull back operation has been confirmed to be rather small (De Oliveira et al., 2013; Rossi et al., 2014; Sahli Costabal et al., 2017; Whiteley et al., 2007) (which somewhat justifies the search for other means of describing MEF mechanisms). It is clear that further understanding in this regard is required, possibly using dedicated experimental approaches via fluorescence optical mappings. However these techniques still require advancements of more sophisticate motion tracking algorithms.

Processes related to MEF have a fundamental role in a wide variety of *passive* physical systems. Notable examples comprise corrosion (Zheng et al., 2015), rock anisotropy (Johnson and Rasolofosaon, 1996), glass transition (Cohen, 1989), dissolution phenomena (Miller-Chou and Koenig, 2002), electromigration (Wang and Suo, 1997), hydrogen trapping (Chêne, 2008), as well as swelling effects (Hong et al., 2009). Clear evidence for the existence of such a coupling in biological systems has also been recently observed in strain-dependent oxygen diffusivity in cartilage (Jackson et al., 2009; Yuan et al., 2009), and in transcription factors within the cell nucleus (Nava et al., 2016). Regarding the specific context of active biological media, connections forming gap junctions in cardiomyocytes (and associated to intercellular communication and mesoscale diffusion) have been recently discussed in terms of their mechano-sensitive properties (Salamhe and Dhein, 2013). Furthermore, a quantitative analysis on the specific effects of stretch into connexins in terms of hemichannels has been experimentally verified in a number of different cellular preparations (Bao et al., 2004; Cherian et al., 2005).

In the perspective of the present work, an important number of experimental studies have demonstrated key MEF effects in ventricular myocardium and atrial tissue (see e.g. Quinn et al., 2014; Ravelli, 2003 for an extended review). Specific applications include atria arrhythmias, where basically three main results are available. First, the spatiotemporal distribution of atrial excitation depends strongly on the anatomical substrate (Ravelli et al., 2005). Secondly, upon mechanical loading (stretching), the conduction velocity of the excitation wave decreases, a beat-to-beat interval variability appears, early afterdepolarisations, ectopic excitations and a higher vulnerability to atrial fibrillation are present (Masé and Ravelli, 2008). Third, atrial tissue undergoes multiple high frequency and unstable rotors (spiral waves) when subject to constant and variable stretch states (Yamazaki et al., 2009). Experimental evidence of MEF has also been studied during ventricular loading, indicating a strong relationship between variations in the conduction velocity and strain anisotropy (De Oliveira et al., 2015; Franz et al., 1989; Lab, 1978; Mills et al., 2011).

The fact that electrical properties of solids undergo intrinsic modifications due to (even infinitesimal) deformations has been a subject of study since several decades (see e.g. the classical volume by Landau et al. on the electrodynamics of continuous media (Landau et al., 1984, pp. 69)). These changes suggest the representation of the corresponding models using strain-dependent (or also stress-dependent) dielectric tensors. In particular, this dependency in turn affects the electromagnetic dynamics by enforcing inhomogeneous and anisotropic patterns in structures that were not necessarily so. Experimental evidence supports the main present assumption that electrical conductivity (hereafter referred as diffusion for the case at hand) depends on deformation. Therefore, and thanks to first principles, one can readily Taylor-expand a given diffusion tensor in terms of the deformation quantities.

In this note we present a novel formulation for the description of soft active deformable media within the context of coupled reaction-diffusion-mechanics systems, and employ nonlinear cardiac dynamics as a main motivating example. At this point we highlight that the concept of stress-assisted diffusion has been originally formulated for generalised composite media (see Aifantis, 1980; Klepach and Zohdi, 2014; Miehe et al., 2014; Weitsman, 1987 and the references therein), but many resemblances exist with respect to the active deformation of soft tissues (De Vita et al., 2017). Most notably, here we have found that an anisotropic and inhomogeneous diffusivity is naturally induced by mechanical deformations, thus affecting the nonlinear dynamics of the spatiotemporal excitation wave. This important fact implies that the present formulation can recover and generalise a large class of electromechanical models based on basic FitzHugh-Nagumo-type descriptions (Aliev and Panfilov, 1996; Panfilov and Keldermann, 2005). The most relevant additional parameters are here the weights accompanying the stress when incorporated into the diffusion tensors, and therefore we study the plausibility of specific choices in the model parameter space. Our assessment is conducted for stretched tissues, focusing on appropriate physical indicators as conduction velocity, propagation patterns and spiral dynamics, and also carefully identifying conditions leading to the stability of the coupled system.

2. A stress-assisted electromechanical model

We centre our investigation on an active stress RD model describing qualitative non-oscillatory properties of cardiac tissue supporting stable propagation of excitation waves (Nash and Panfilov, 2004; Panfilov and Keldermann, 2005). We frame our modelling into finite elasticity, where one identifies the relationship between material (reference) and spatial (deformed) coordinates, indicated by X_I and x_j, respectively, via the smooth map $x_j(X_I)$ that determines then the deformed position of a point x_j originally located at X_I. We indicate with J the Jacobian of the map. In the deformed configuration the proposed equations read:

$$\frac{\partial V}{\partial t} = \frac{\partial}{\partial x_i} d_{ij}(\sigma_{ij}) \frac{\partial V}{\partial x_j} + I_{\text{ion}}, \quad \frac{\partial r}{\partial t} = f(V, r)\,, \tag{2.1}$$

$$\frac{\partial T_a}{\partial t} = \epsilon(V)(k_{T_a} V - T_a), \quad \frac{\partial \sigma_{ij}}{\partial x_i} = 0\,, \tag{2.2}$$

with constitutive prescriptions for the RD system (Panfilov and Keldermann, 2005)

$$I_{\text{ion}} = -kV(V-a)(V-1) - rV\,, \tag{2.3a}$$

$$f(V, r) = \left(\eta + \frac{\mu_1 r}{\mu_2 + V}\right)(-r - kV(V - b - 1))\,, \tag{2.3b}$$

and for incompressible isotropic materials ($J = 1$)

$$\sigma_{ij} = 2c_1 b_{ij} - 2c_2 b_{ij}^{-1} - p\delta_{ij} + T_a \delta_{ij}\,, \tag{2.4}$$

$$d_{ij}(\sigma_{ij}) = D_0 \delta_{ij} + D_1 \sigma_{ij} + D_2 \sigma_{ik}\sigma_{kj}\,. \tag{2.5}$$

Eq. (2.1) provides a non-dimensional, two-variables RD model where V represents the transmembrane potential and r is the recovery variable, whose dynamics is prescribed by Eqs. (2.3). The term $kV(V-a)(V-1)$ controls the fast processes regulated via the

Table 1
Model parameters specifying the phenomenological RD cardiac dynamics and the active-stress mechanics (2.1)–(2.5), where D_0 is a non-dimensional diffusion coefficient, and c_1, c_2 have units of [kPa].

$\Omega = (0, 250)^2$, $a = 0.1$, $b = 0.15$, $k = 8$, $\eta = 0.001$, $\epsilon_0 = 0.1$, $\mu_1 = 0.12$, $\mu_2 = 0.3$, $k_{Ta} = 9.58$, $c_1 = 6$, $c_2 = 2$, $D_0 = 1$, $V_{\text{init}} = 0$, $r_{\text{init}} = 0.4$, $(T_a)_{\text{init}} = 0.2$, D_1, D_2 from Fig. 1(a)

threshold parameter a, while recovery and restitution properties are determined via the phenomenological parameters k, μ_1, μ_2, b, having no particular physical meaning (cf. Nash and Panfilov, 2004).

Eq. (2.2) provides the contractile (active stress) dynamics of the tissue and the balance of linear momentum (law of motion). The constant k_{Ta} modulates the amplitude of the active stress, while $\epsilon(V)$ is a Heaviside function introducing a discontinuous coupling (a switch) with the dynamics of the voltage (Nash and Panfilov, 2004): $\epsilon(V) = \epsilon_0$ if $V < 0.05$, and $\epsilon(V) = 10\epsilon_0$ if $V \geq 0.05$.

Eq. (2.4) provides the total equilibrium stress in the current deformed configuration (σ_{ij} is the Cauchy stress (Spencer, 1989)). Such a formulation highlights the two main contributions due to the multiscale behaviour of the tissue, i.e. (i) the passive stress component originating from the classical strain energy function adopted for incompressible Mooney-Rivlin materials (Ogden, 1997) and (ii) the active stress component following the formulation proposed in Nash and Panfilov (2004), contributing as an additional hydrostatic term to the total stress tensor only. The second order tensors δ_{ij} and b_{ij} are the identity and left Cauchy-Green strain (Spencer, 1989), respectively. Model parameters are provided in Table 1.

Eq. (2.5) introduces the stress-assisted diffusion equation, adapting the ideas in Aifantis (1980), to describe in our case a generalisation of the effects of tissue deformation on action potential spread for isotropic and incompressible nonlinear elastic solids. The parameter D_0 is the non-dimensional diffusion coefficient, while D_1 and D_2 parameterise the effect of the mechanical stress on the diffusive flux.

We remark that the present coupling is motivated by the phenomenon of dilute solutes in a solid matrix. In our context, this process is clearly similar to the propagation of voltage membrane within the cardiac tissue. The theory, generalising the Fick's phenomenological description of diffusion, uses the classical Euler's axioms of continuously distributed matter allowing one to impose the balance of momentum and to ensure frame invariance (Tadmor et al., 2012). Accordingly, we assume the membrane voltage as a continuum field undergoing slow diffusion on a macroscopically rigid matrix that, in fact, is considered at equilibrium at each fixed time (the usual quasi-static condition). Therefore, the macroscopic response results independent on the diffusion process while the diffusion process strongly depends on the mechanical state. This specific theoretical result allows us to selectively introduce the two known physical couplings in the cardiac electromechanical modelling, i.e. the effect of the mechanical state on (1) the excitation state (stretch-activated currents) and (2) the diffusion process (stress-driven anisotropy). In view of the objectives of the present study, we do not consider here stretch-activated currents (as introduced in Panfilov and Keldermann, 2005), and follow instead the treatment in Nash and Panfilov (2004).

According to the representation formula for isotropic second order tensors (Spencer, 1989), the diffusive flux accounts for hydrostatic stress effects on the diffusing species and is characterised by three contributions: $D_0\delta_{ij}$ recovering the classical linear diffusion equation for a homogeneous and isotropic medium (Nash and Panfilov, 2004), while $D_1\sigma_{ij}$ and $D_2\sigma_{ik}\sigma_{kj}$ allow for stress-induced anisotropies into the diffusion tensor (this part is associated to the theory by Landau et al. (1984) for infinitesimal deformations). Eq. (2.5) further represents an isotropic tensor function thus implying that the eigenvectors of σ_{ij} and d_{ij} coincide. This particular aspect is investigated and visualised in the following numerical tests.

3. Numerical results

Numerical method. The discretisation of (2.1)–(2.5) follows the mixed-primal finite element formulation proposed in Ruiz-Baier (2015), where strains and stresses are computed directly without postprocessing them from low-order discrete displacements. This approach is preferable in the present context as we aim at analysing properties of the stress and diffusion tensors directly. Consequently, stresses are approximated with row-wise lowest order Raviart-Thomas elements (Raviart and Thomas, 1977), displacements with stabilised Brezzi-Douglas-Marini elements of degree one (Brezzi et al., 1985), whereas pressure (if actually needed) can be recovered from the discrete stress. The remaining fields (transmembrane potential, recovery variable, and active tension) are approximated with continuous, piecewise linear elements. We employ unstructured triangular meshes of different resolutions, and we set a fixed time step $\Delta t = 10^{-3}$. The solver consists of an outer time advancing loop (of first order backward Euler type), an embedded fixed point iteration to decouple the electrophysiology RD system from the finite elasticity discrete equations, and inner Newton steps for the solution of the nonlinear mechanics. In turn, the action potential model (2.1) is solved semi-implicitly (taking only the reaction terms explicitly), determining a formal CFL condition associated to the finest mesh and supporting the choice of the timestep mentioned above. All linear solves are carried out with a PETSc built-in LU solver using ILU factorisation as preconditioner.

Parameter space. In order to determine admissibility regions for the modified RD system, we conduct an inspection of the parabolicity regimes depending on the model parameters (see e.g. Showalter, 1979). Let us first consider a uniaxial tensile configuration of a two-dimensional domain where we induce a target pattern (see Fig. 2(b), left) and identify horizontal (X_0, X_1) and vertical (Y_0, Y_1) positions. Fixing the stretching of the domain at the maximum physiological level for cardiac tissue, i.e. 20% of the resting length, one can obtain the maximum tensile components and a diagonal form of the Cauchy stress tensor can be readily derived in the central uniform tensile region (Ogden, 1997), i.e.:

$$[\sigma_{ij}] = \begin{bmatrix} \sigma_1 & 0 \\ 0 & \sigma_2 \end{bmatrix}, \qquad [\sigma_{ik}\sigma_{kj}] = \begin{bmatrix} \sigma_1^2 & 0 \\ 0 & \sigma_2^2 \end{bmatrix},$$

where σ_1, σ_2 correspond to the eigenvalues of the stress tensor that overlap with the two diagonal components of the stress in the Cartesian coordinate system, i.e., σ_{11}, σ_{22}. Accordingly, the generalised diffusion tensor (2.5) becomes

$$[d_{ij}] = \begin{bmatrix} 1 + D_1\sigma_1 + D_2\sigma_1^2 & 0 \\ 0 & 1 + D_1\sigma_2 + D_2\sigma_2^2 \end{bmatrix},$$

where a second order polynomial expression is obtained and parameterised over the two coefficients D_1, D_2. We can then readily identify the regimes where the modified conductivity is a positive definite tensor. This translates in requiring that the graph of $d_{11} \equiv d_{22} = 1 + D_1\sigma + D_2\sigma^2$ is always positive, or equivalently

$$4D_2 > D_1^2,$$

thus implying convexity and no real roots. Such a condition also ensures that both tensile and compressive states are physically allowed according to the material response without compromising the uniform parabolicity of the differential operator defining $(2.1)_1$.

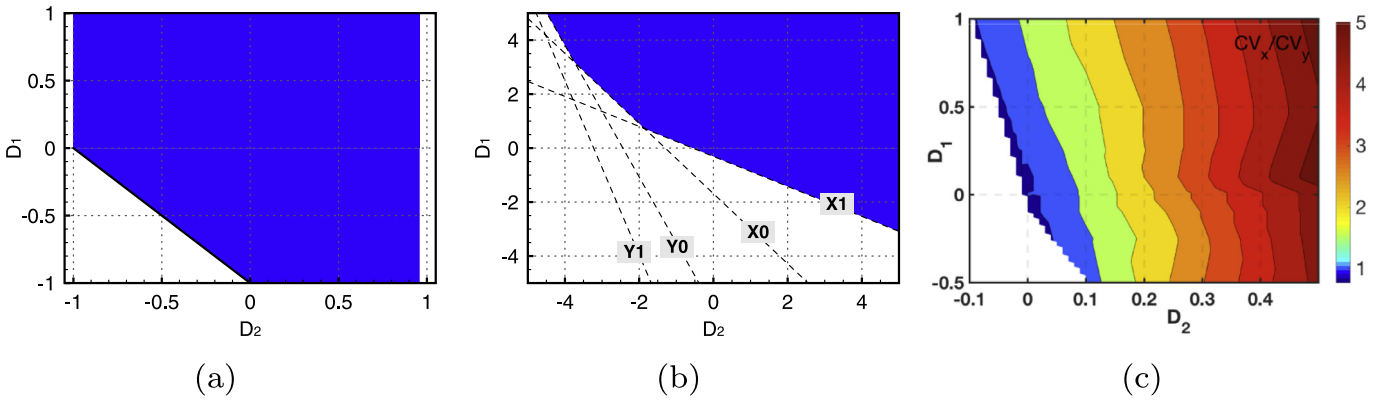

Fig. 1. Parameter space. Conditions for parabolicity of the generalised diffusion tensor (2.5): (a) theoretical normalised case for unitary stress ($\sigma_1 = \sigma_2 = 1$); (b) computed stress values at locations X_0, X_1, Y_0, Y_1 during uniaxial loading, (c) numerical conduction velocity ratio between horizontal CV_x, (X_0, X_1 locations), and vertical CV_y, (Y_0, Y_1 locations), computed during target pattern stimulation in Fig. 2(b).

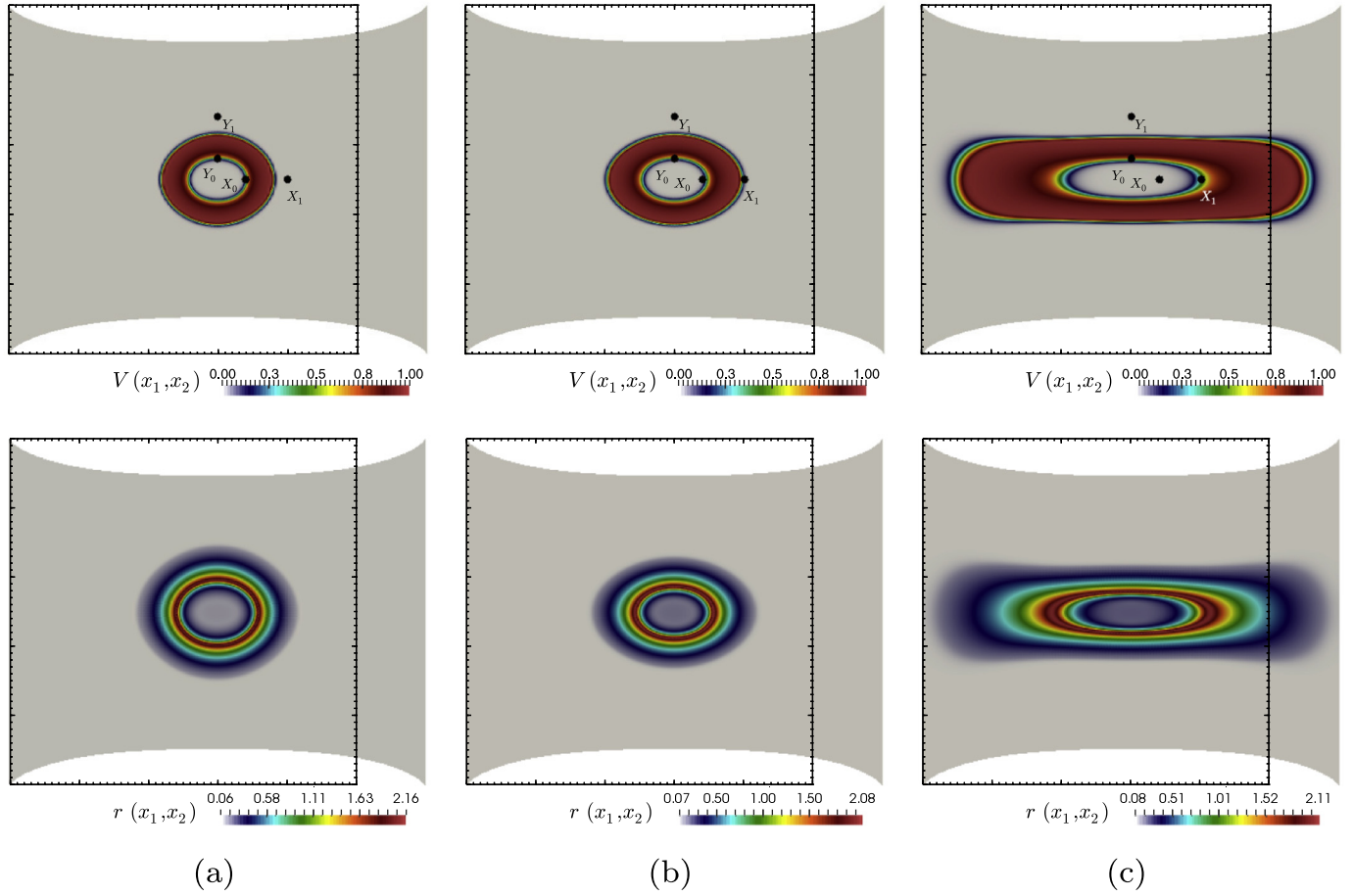

Fig. 2. Stress-induced anisotropy. Target pattern simulation with $D_1 = D_2 = 0$ according to Nash and Panfilov (2004) (a), $D_1 = -0.01, D_2 = 0.01$ (b) and $D_1 = -0.25, D_2 = 0.25$ (c). Locations (X_0, Y_0, X_1, Y_1) refer to the horizontal and vertical directions used to compute the corresponding conduction velocities CV_x, CV_y. Top panels show the electric potential and the bottom row presents the distribution of the recovery variable.

After fixing $D_0 = 1$, we proceed to characterise the theoretical parameter space for an idealised tensile state ($\sigma_1 = \sigma_2 = 1$). Fig. 1(a) displays the region plot of the map $d_{11} = 1 + D_1 + D_2$, highlighting in blue colour the admissible regions where parabolicity holds. On the other hand, we perform numerical simulations (with stresses σ_1, σ_2) and extract the computed values of the stresses at selected locations (X_0, Y_0, X_1, Y_1) whose parabolicity conditions obtained via the map d_{11} are shown in Fig. 1(b). Finally, the physical parameter space is derived directly from numerical simulations for the same uniaxial condition in Fig. 1(c). We compute the conduction velocities of the generated wave along the selected locations, CV_x, CV_y, and identify regions with loss of parabolicity when the travelling waves present a propagation fault (non coloured region). In particular, the produced values of CV_x/CV_y are for the most larger than 1 since the mechanical stretching is applied in the $x-$direction and the computations are non-diverging for most positive parameter values. Close to the region $D_1 = D_2 = 0$, the CV ratio is ~ 1, thus recovering the conduction velocity ex-

pected for an isotropic medium (that is, the same independently of the direction). Particular combinations with D_1 or $D_2 < 0$ are characterised by $CV_x/CV_y < 1$ thus implying a reduction of the conduction velocity in the direction of stretching (see regions in blue, in Fig. 1(c)). In contrast, for larger positive parameter values the wave moving in the $x-$direction propagates much faster than the one in the $y-$direction (up to a fivefold in our analyses). In all the selected scenarios, the analysis clearly indicates a marked anisotropic effect on the diffusion process, due to stress.

We point out that the parametric analysis conducted in this section is only aimed at characterising parabolicity regions of the differential equations endowed with the new constitute law. Different choices of the parameters D_1, D_2 are explored in this phenomenological context; but we stress that a more precise interpretation and tuning of these parameters deserves further investigation, especially from physical and chemical perspectives based on experimental observations.

Stress-induced anisotropy. Fig. 2 shows three representative examples of different levels of the stress- induced anisotropic coupling. One can observe how the propagating behaviour is modified by the level of anisotropy induced on the tissue, initially homogeneous and isotropic, thanks to the stress-assisted mechanism. Based on the selected parameters, a faster propagation is obtained in the direction of loading where a horizontal uniaxial stress state is induced. In the first case (corresponding to Fig. 2(a)), the choice $D_1 = D_2 = 0$ does not induce any effect on the excitation wave and the only visual difference is due to the geometric mapping from the reference to the deformed configuration of the computational domain. Actually, this setting (which is the expected behaviour in the classical active stress approach for incompressible isotropic materials (Nash and Panfilov, 2004)) is the most commonly employed in models and simulations for the electromechanical coupling and it has been shown to have a limited effect (De Oliveira et al., 2013; Sahli Costabal et al., 2017; Whiteley et al., 2007), but using other models and constitutive assumptions. The second case (see Fig. 2(b)) is characterised by $D_1 = -0.01, D_2 = 0.01$ (representing a small coupling of the stress-assisted diffusion) and shows a mild, though significative, anisotropic effect due to the applied mechanical stretching in the horizontal direction. The obtained behaviour is the one expected based on the few cardiac optical mapping data describing such a phenomenon in a moving frame (Miller-Chou and Koenig, 2002) and, out of these three cases, it is qualitatively the most appropriate, in terms of physiological behaviour of cardiac dynamics.

The last run (see Fig. 2(c)) uses larger values $D_1 = -0.25, D_2 = 0.25$, and our results produce a CV_x about a threefold higher than CV_y. This particular test points out a critical example of the effect of mechanical stretching on the diffusive properties of the species in terms of transmembrane potential V (top panels) and recovery variable r (lower panels). The observed level of distortion induced on the excitation wave may be expected in some pathological scenarios with drastically compromised excitation-contraction dynamics (O'Rourke et al., 1999). We remark that this analysis is of particular importance in the study of the effects of the electromechanical coupling into spiral wave drifting phenomena and atrial arrhythmias.

Stress-induced arrhythmogenesis. Additional effects on arrhythmogenesis are exemplified with a simulation of sustained spiral dynamics. Fig. 3 compares the long run behaviour of an equally induced spiral within a uniaxially stretched tissue for three increasing levels of the stress-assisted diffusion parameters D_1 and D_2. For the chosen parameters' set from the original model a stationary circular meander pattern is expected (Fig. 3(a)), although spiral drifting is observed as the stress-assisted diffusion is activated (Fig. 3(b)). In addition, totally distorted excitation waves are observed when a very strong stress-induced anisotropic coupling is enforced (Fig. 3(c)) via higher values of the parameters D_1 and D_2. The corresponding recovery variable is also provided and confirms the highlighted differences (Fig. 3(d)–(f)).

The analysis is further quantified by rendering the modified diffusion tensors in terms of their *tensorial glyph* representation (see e.g. Ennis et al., 2005). These plots (see Fig. 4) are generated by solving local eigenvalue problems using the tensor at hand and displaying an ellipsoid whose shape and size determine the magnitude of eigenvalues and direction of eigenvectors and indicating the local patterns of anisotropy and inhomogeneity. For reference, we also depict the L^2-norm of the resulting diffusion tensor in each case, that is $D_0 C_{IJ}^{-1}$, D_{IJ}, and S_{IJ}, respectively. As expected, constant diffusion, Fig. 4(a), and stress-assisted diffusion, Fig. 4(b), lead to different representations of the eigenproblem. In particular, close to the boundary of the domain, different eigendirections are observed. This behaviour also suggests an influence of local stresses into diffusion. Even if we only account for the uniaxial case (represented in Fig. 4(c)), substantial differences are expected when multiaxial stress patterns are considered.

According to Panfilov and Keldermann (2005), when stretch-activated currents are present, we observe a *small* spiral drift velocity of about 1.4% variation with respect to pulse wave velocity. This means that several spiral rotations are required to reach the boundary of the domain such to detect the exit of the excitation wave from the domain (auto-defibrillation). However such small differences can lead to substantially different scenarios at long times, as observed in strongly nonlinear dynamical systems (Bueno-Orovio et al., 2016; Hurtado et al., 2016). This behaviour is in line with the expected vulnerability to atrial flutter and atrial fibrillation during atrial dilatation (Masé and Ravelli, 2008; Ravelli et al., 2005; Yamazaki et al., 2009). At this stage we remark that our theoretical study does not imply a stretch-activated current contribution (still debated in the literature (Quinn et al., 2014)) but only relies on the effect induced by the generalised diffusivity tensor.

Enhanced effects due to mechanical pacing. Finally we carry out a set of simulations of the fully coupled stress-assisted diffusion model, concentrating in the case where a periodic and uniaxial mechanical loading is applied on the right end of the square slab $\Omega = (0, 250)^2$. Again, the material and electrical parameters are taken from Table 1, concentrating in the case of adimensional units. The boundary conditions for the nonlinear elasticity problem correspond to zero normal stresses on the horizontal boundaries, a clamped left boundary, and on the right we prescribe the displacement

$$\mathbf{u} = \left[50 \sin^2\left(\frac{\pi}{50}[t - t^*]\right),\ 0\right]^T,$$

where $t^* = 100$ indicates the onset time for the mechanical loading. We use a S1-S2 protocol to initiate spiral wave dynamics, and focus our attention on the long term behaviour of the patterns produced according to three different levels of stress-assisted diffusion. In Fig. 5 we portray the trajectory of the spiral tip (also showing a zoom on the relevant region) over the time interval $t \in [400, 1000]$. The location of the spiral tip is recorded by computing a piecewise constant field defined as the module of the gradient of the recovery variable, and then obtaining its global argmax over the spatial domain. Our results indicate a marked progressive drifting of the spiral tip, which increases as the relevant parameters depart from the stable values and induce a high level of the stress-induced anisotropy.

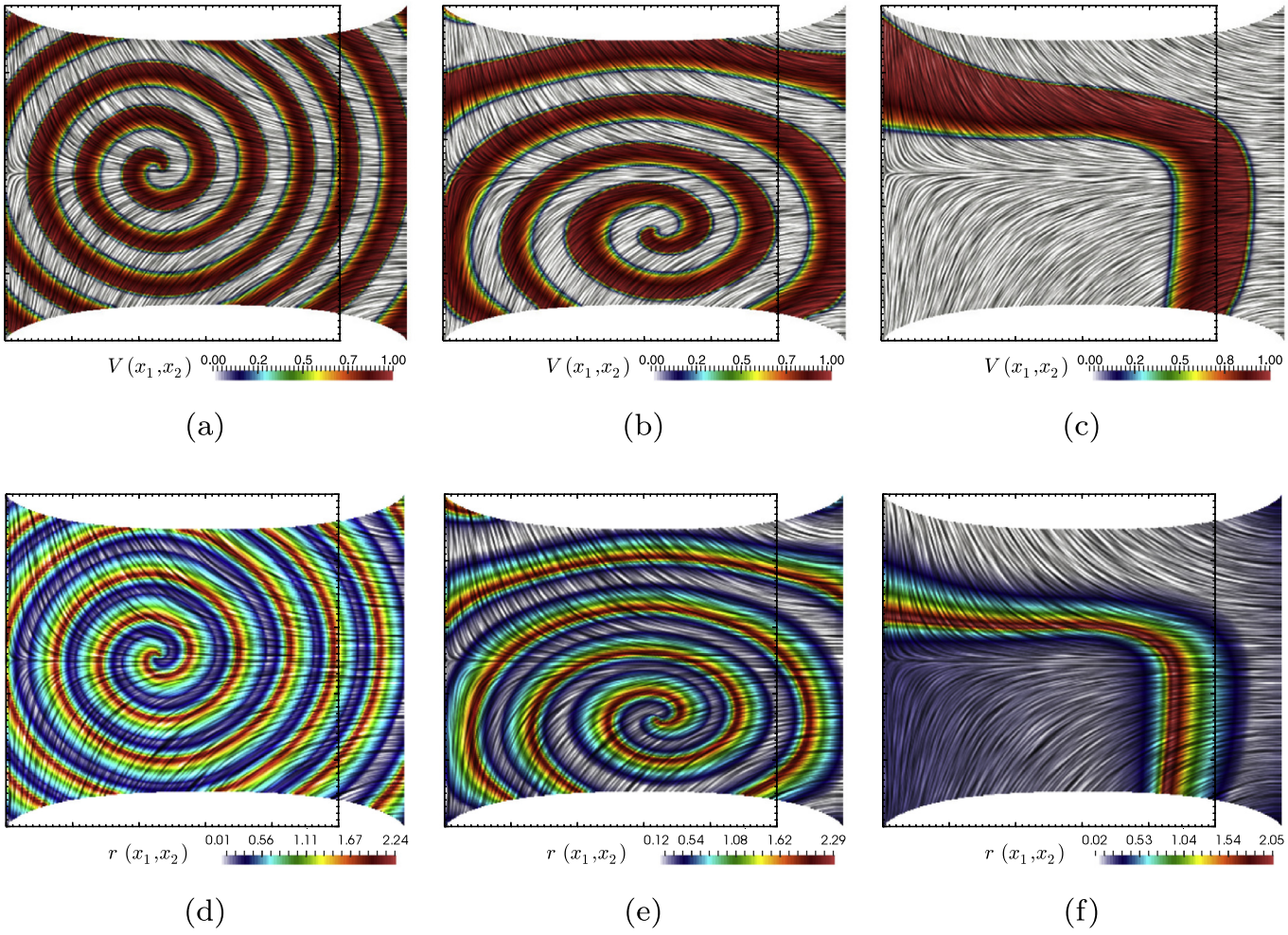

Fig. 3. Stress-induced arrhythmogenesis. Comparison of spiral dynamics induced by (a,d) constant diffusion according to Nash and Panfilov (2004) and to Piola transformation (i.e. $D_0 C_{ij}^{-1}$), and those generated by stress-assisted diffusion with $D_1 = -0.015, D_2 = 0.015$ (b,e) and $D_1 = 0.15, D_2 = 0.015$ (c,f). The action potential distribution V is shown in panels (a,b,c) and the recovery variable distribution r is presented in panels (d,e,f).

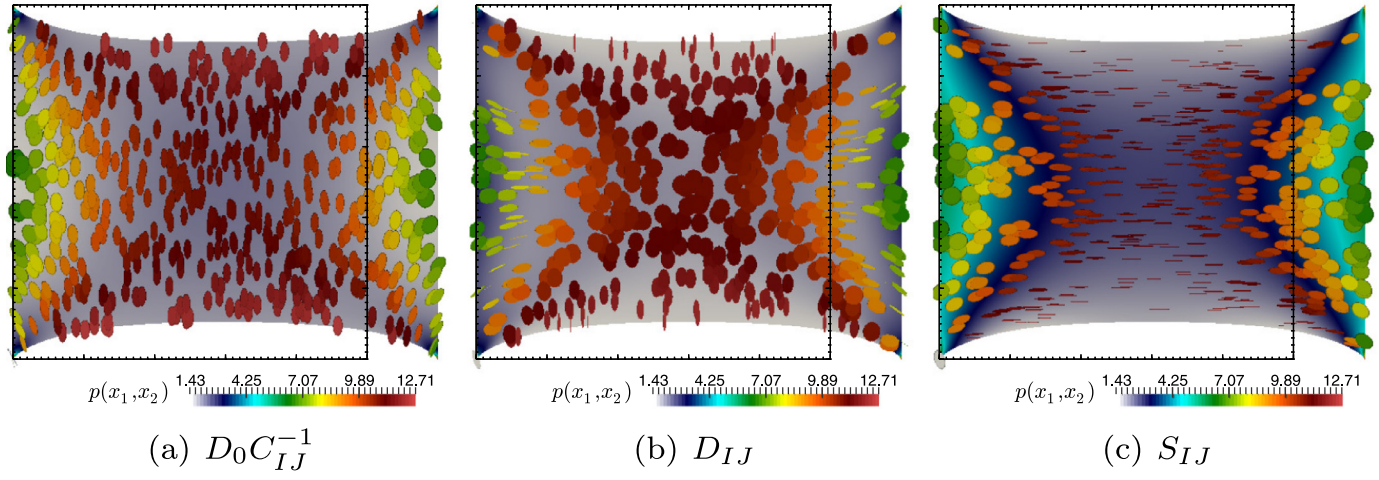

Fig. 4. Stress-induced arrhythmogenesis. Tensorial glyphs representation with pressure values for the anisotropic and inhomogeneous diffusion induced by the Piola transformation only (a) and by the stress-assisted diffusion using $D_1 = -0.15, D_2 = 0.015$ (b). Panel (c) shows the anisotropy of the second Piola-Kirchhoff tensor. Ellipsoids with diverse sizes and shape ratios indicate a high anisotropic degree. The colour-bars indicate the pressure on the tensorial glyphs, whereas the field plotted in the back is the L^2-norm of each diffusion tensor.

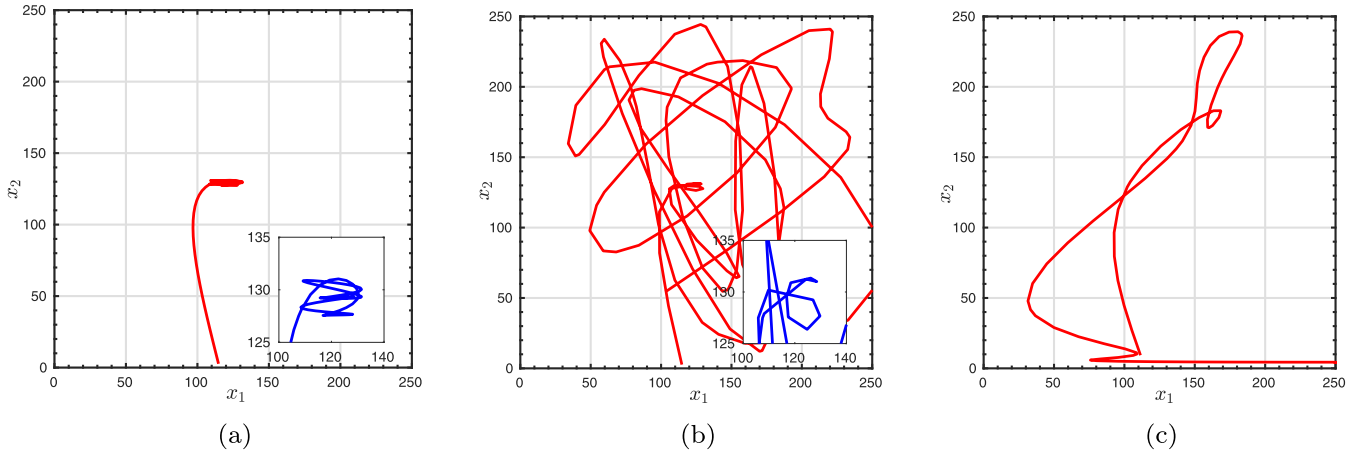

Fig. 5. Enhanced effects due to mechanical pacing. Trajectories of the spiral tip depending on three different stress-assisted diffusion configurations. $D_1 = -0.015, D_2 = 0.015$ (a), $D_1 = 0.275, D_2 = -0.275$ (b), and $D_1 = -0.5, D_2 = 0.5$ (c). The inset plots indicate a zoom of each trajectory near the meandering location at larger times.

4. Discussion

In this work we propose a generalised MEF formulation for active deformable media based on the concept of stress-assisted diffusion. The leading mechanism of the modification of wave propagation corresponds to the introduction of anisotropy in an originally isotropic medium. In this study, we simulated a single spiral wave that drifts or degenerates according to the amount of stress-assisted coupling. The proposed physics, experimentally and theoretically based on physical grounds, enriches the phenomenological description of electro-mechanical RD systems in the context of cardiac dynamics and excitable deformable media in general. The numerical results confirm that the generalised formulation induces anisotropy in the wave propagation starting from an isotropic medium. Secondly, the RD dynamics are modified, as clearly evidenced by the change in spiral meandering (i.e. drift of the spiral tip (Nash and Panfilov, 2004; Panfilov and Keldermann, 2005)). In addition, the generalised model leads to inhomogeneous and unpredicted excitation waves, especially pronounced for extreme values of the coupling coefficients as observed in long run tests and under mechanical pacing. We deliberated choose not to consider stretch-activated currents in this contribution since our object was to emphasize the sole role of complex diffusive effects. Accordingly, no extra excitations are induced by the mechanical state on the action potential behavior. We in fact foresee to incorporate and investigate the two physical couplings in forthcoming contributions.

To close this section we collect a few possible extensions of this work. The connection between spatio-temporal variation of the tissue anisotropy and the identification of model parameters in general cases remains unclear, but it is by no means a trivial task (Dorfmann et al., 2017; Namy et al., 2004). One would definitely require to analyse deformation patterns interacting with a number of intrinsic properties (not considered here) as domain curvature, a priori anisotropy, pre-stretch, structural heterogeneities, and many others.

Also, we would be interested in analysing important microscopic effects related to gap junction proteins density at cell-cell interfaces (Jacquement and Henriquez, 2008; Lenarda et al., 2017; Ronan et al., 2015). These properties have an important effect on the macroscopic diffusivity and its relation with the conduction velocity (Thomas et al., 2003), especially under pathological remodelling conditions. Major effects on conduction velocity are also due to thermo-electric couplings, that can be directly introduced in the present theoretical formulation (Fenton et al., 2013; Gizzi et al.). Other envisaged modifications include different mechanical constraints (Land et al., 2017; McCain et al., 2012), the incorporation of beat-to-beat adaptation (see the recent review (Quinn and Kohl, 2016)) as well as multiscale calcium ions effects triggering delayed afterdepolarizations (Ko et al., 2017).

An important complement to our generalised MEF formulation would be the characterisation of admissibility ranges for an elementary mechanical setup, together with the experimental validation of the proposed model. The latter could be carried out by fine-tuning stress-assisted diffusion parameters via optical mapping of cell cultures, myocardial tissue slices, and whole heart geometries (with particular attention to atrial tissue).

Several other applications are foreseen, as stretch-activated currents and MEF in cell-cell coupling phenomena. However a deeper understanding of the interacting regimes (also including model parameters and biophysical descriptions) is still required before engaging in the study of these mechanisms using homogenisation theory.

Acknowledgements

This work has been partially supported by the Italian National Group of Mathematical Physics GNFM-INdAM, by the International Center for Relativistic Astrophysics Network ICRANet, by the London Mathematical Society through their Grant Scheme 4, and by the EPSRC through the Research Grant EP/R00207X/1. We also thank the valuable inputs from two anonymous referees, leading to substantial improvement with respect to the original manuscript.

References

Aifantis, E.C., 1980. On the problem of diffusion in solids. Acta Mech. 37, 265–296.
Aliev, R.R., Panfilov, A.V., 1996. A simple two-variable model of cardiac excitation. Chaos Solitons Fractals 7, 293.
Bao, L., Sachs, F., Dahl, G., 2004. Connexins are mechanosensitive. Am. J. Physiol. - Cell Physiol. 287 (5), C1389–C1395.
Brezzi, F., Douglas, J., Marini, L.D., 1985. Two families of mixed finite elements for second order elliptic problems. Numerische Mathematik 47 (2), 217–235.
Bueno-Orovio, A., Teh, I., Schneider, J.E., Burrage, K., Grau, V., 2016. Anomalous diffusion in cardiac tissue as an index of myocardial microstructure. IEEE Trans. Med. Imaging 35, 2200–2207.
Chen, D.D., Gray, R.A., Uzelac, I., Herndon, C., Fenton, F.H., 2017. Mechanism for amplitude alternans in electrocardiograms and the initiation of spatiotemporal chaos. Phys. Rev. Lett. 118, 168101.
Chêne, J., 2008. Strain-assisted transport of hydrogen and related effects on the intergranular stress corrosion cracking of alloy 600. Environment-Induced Cracking of Materials. Elsevier Ltd.

Cherian, P.P., Siller-Jackson, A.J., Gu, S., Wang, X., Bonewald, L.F., Sprague, E., Jiang, J.X., 2005. Mechanical strain opens connexin 43 hemichannels in osteocytes: a novel mechanism for the release of prostaglandin. Mol. Biol. Cell 16 (7), 3100–3106.

Cherubini, C., Filippi, S., Nardinocchi, P., Teresi, L., 2008. An electromechanical model of cardiac tissue: constitutive issues and electrophysiological effects. Prog. Biophys. Mol. Biol. 97, 562–573.

Cohen, D.S., 1989. Sharp fronts due to diffusion and stress at the glass transition in polymers. J. Polymer Sci. 27, 1731–1747.

Das, N.P., Mahanta, D., Dutta, S., 2014. Unpinning of scroll waves under the influence of a thermal gradient. Phys. Rev. E 90, 022916.

De Oliveira, B.L., Pfeiffer, E.R., Joakim, S., Wall, S.T., McCulloch, A.D., 2015. Increased cell membrane capacitance is the dominant mechanism of stretch-dependent conduction slowing in the rabbit heart: a computational study. Cell. Mol. Bioeng. 8, 237–246.

De Oliveira, B.L., Rocha, B.M., Barra, L.P.S., Toledo, E.M., Sundnes, J., Weber dos Santos, R., 2013. Effects of deformation on transmural dispersion of repolarization using in silico models of human left ventricular wedge. Int. J. Numer. Methods Biomed. Eng. 29, 1323–1337.

De Vita, R., Grange, R., Nardinocchi, P., Teresi, L., 2017. Mathematical model for isometric and isotonic muscle contractions. J. Theor. Biol. 425, 1–10.

Dorfmann, L., Saccomandi, G., Salvatori, M.C., 2017. On the use of universal relations in modeling nonlinear electro-elastic materials. Int. J. Mech. Sci. In Press.

Ennis, D.B., Kindlman, G., Rodriguez, I., Helm, P.A., McVeigh, E.R., 2005. Visualization of tensor fields using superquadric glyphs. Magn. Reson. Med. 53 (1), 169–176.

Fenton, F.H., Gizzi, A., Cherubini, C., Pomella, N., Filippi, S., 2013. Role of temperature on nonlinear cardiac dynamics. Phys. Rev. E 87, 042709.

Franz, M.R., Burkhoff, D., Yue, D.T., Sagawa, K., 1989. Mechanically induced action potential changes and arrhythmia in isolated and in situ canine hearts. Cardiovasc. Res. 23, 213–223.

Gizzi, A., Cherubini, C., Filippi, S., Pandolfi, A., 2015. Theoretical and numerical modeling of nonlinear electromechanics with applications to biological active media. Commun. Comput. Phys. 17, 93–126.

Gizzi, A., Loppini, A., Ruiz-Baier, R., Ippolito, A., Camassa, A., La Camera, A., Emmi, E., Di Perna, L., Garofalo, V., Cherubini, C., Filippi, S., In Press. Nonlinear diffusion & thermo-electric coupling in a two-variable model of cardiac action potential. Chaos.

Hong, W., Liu, Z., Suo, Z., 2009. Inhomogeneous swelling of a gel in equilibrium with a solvent and mechanical load. Int. J. Solids Struct. 49, 3282–3289.

Hurtado, D.E., Castro, S., Gizzi, A., 2016. Computational modeling of non-linear diffusion in cardiac electrophysiology: a novel porous-medium approach. Comput. Methods Appl. Mech. Eng. 300, 70–83.

Jackson, A.R., Travascio, F., Hu, W.Y., 2009. Effect of mechanical loading on electrical conductivity in human intervertebral disc. J. Biomech. Eng. 131, 054505.

Jacquement, V., Henriquez, C.S., 2008. Loading effect of fibroblast-myocyte coupling on resting potential, impulse propagation, and repolarization: insights from a microstructure model. Am. J. Physiol. - Heart Circ. Physiol. 294, H2040–H2052.

Johnson, P.A., Rasolofosaon, P.N.J., 1996. Nonlinear elasticity and stress-induced anisotropy in rock. J. Geophys. Res. 101, 3113–3124.

Kaufmann, R., Theophile, U., 1967. Automatic-fordernde dehnungseffekte an purkinje-faden, pappillarmuskeln und vorhoftrabekeln von rhesus-affen. Pflugers Arch. Gesamte Physiol. Menschen Tiere 297, 174–189.

Klepach, D., Zohdi, T.I., 2014. Strain assisted diffusion: modeling and simulation of deformation-dependent diffusion in composite media. Composites 56, 413–423.

Ko, C.Y., Liu, M.B., Song, Z., Qu, Z., Weiss, J.N., 2017. Multiscale determinants of delayed afterdepolarization amplitude in cardiac tissue. Biophys. J. 112, 1949–1961.

Kohl, P., Sachs, F., 2001. Mechanoelectric feedback in cardiac cells. Philos. Trans. R. Soc. London A 359, 1173–1185.

Lab, M.J., 1978. Mechanically dependent changes in action potentials recorded from the intact frog ventricle. Circul. Res. 42, 519–528.

Land, S., Park-Holohan, S.J., Smith, N.P., Dos Remedios, C.G., Kentish, J.C., Niederer, S.A., 2017. A model of cardiac contraction based on novel measurements of tension development in human cardiomyocytes. J. Mol. Cell. Cardiol. 106, 68–83.

Landau, L.D., Lifshitz, E.M., Pitaevskii, L.P., 1984. Electrodynamics of Continuous Media, 8. Butterworth-Heinemann, Oxford.

Lenarda, P., Gizzi, A., Paggi, M., 2017. A modeling framework for contact, adhesion and mechano-transduction between excitable deformable cells. arXiv:1707.00920.

Masé, M., Ravelli, F., 2008. A model for mechano-electrical feedback effects on atrial flutter interval variability. Bull. Math. Biol. 70, 1326–1347.

McCain, M.L., Lee, H., Aratyn-Schaus, Y., Kléber, A.G., Parker, K.K., 2012. Cooperative coupling of cell-matrix and cell–cell adhesions in cardiac muscle. Proc. Natl. Acad. Sci. 109 (25), 9881–9886.

Miehe, C., Mauthe, S., Ulmer, H., 2014. Formulation and numerical exploitation of mixed variational principles for coupled problems of Cahn–Hilliard-type and standard diffusion in elastic solids. Int. J. Numer. Methods Eng. 99, 737–762.

Miller-Chou, B.S., Koenig, J.L., 2002. A review of polymer dissolution. Prog. Polym. Sci. 28, 1223–1270.

Mills, R.W., Wright, A.T., Narayan, S.M., McCulloch, A.D., 2011. The Effects of Wall Stretch on Ventricular Conduction and Refractoriness in the Whole Heart. Oxford University Press, chapter 25.

Namy, P., Ohayon, J., Tracqui, P., 2004. Critical conditions for pattern formation and in vitro tubulogenesis driven by cellular traction fields. J. Theor. Biol. 227, 103–120.

Nash, M.P., Panfilov, A.V., 2004. Electromechanical model of excitable tissue to study reentrant cardiac arrhythmias. Prog. Biophys. Mol. Biol. 85, 501–522.

Nava, M.M., Fedele, R., Raimondi, M.T., 2016. Computational prediction of strain-dependent diffusion of transcription factors through the cell nucleus. Biomech. Model. Mechanobiol. 15, 983–993.

Nobile, F., Ruiz-Baier, R., Quarteroni, A., 2012. An active strain electromechanical model for cardiac tissue. Int. J. Numer. Methods Biomed. Eng. 28, 52–71.

Ogden, R.W., 1997. Non-Linear Elastic Deformations. Dover Publications.

O'Rourke, B., Kass, D.A., Tomaselli, G.F., Kääb, S., Tunin, R., Marbán, E., 1999. Mechanisms of altered excitation-contraction coupling in canine tachycardia-induced heart failure, i experimental studies. Circul. Res. 84, 562–570.

Panfilov, A.V., Keldermann, R.H., 2005. Self-organized pacemakers in a coupled reaction-diffusion-mechanics system. Phys. Rev. Lett. 95, 258104.

Panfilov, A.V., Keldermann, R.H., Nash, M.P., 2007. Drift and breakup of spiral waves in reaction-diffusion-mechanics systems. Proc. Natl. Acad. Sci. 104, 7922–7926.

Quinn, T.A., 2014. The importance of non-uniformities in mechano-electric coupling for ventricular arrhythmias. J. Interv. Card. Electrophysiol. 39, 25–35.

Quinn, T.A., 2015. Cardiac mechano-electric coupling: a role in regulating normal function of the heart? Cardiovasc. Res. 108, 1–3.

Quinn, T.A., Kohl, P., 2013. Combining wet and dry research: experience with model development for cardiac mechano-electric structure-function studies. Cardiovasc. Res. 97, 601–611.

Quinn, T.A., Kohl, P., 2016. Rabbit models of cardiac mechano-electric and mechano-mechanical coupling. Prog. Biophys. Mol. Biol. 121 (2), 110–122.

Quinn, T.A., Kohl, P., Ravens, U., 2014. Cardiac mechano-electric coupling research: fifty years of progress and scientific innovation. Prog. Biophys. Mol. Biol. 115, 71–75.

Ravelli, F., 2003. Mechano-electric feedback and atrial fibrillation. Prog. Biophys. Mol. Biol. 82, 137–149.

Ravelli, F., Faes, L., Sandrini, L., Gaita, F., Antolini, R., Scaglione, M., Nollo, G., 2005. Wave similarity mapping shows the spatiotemporal distribution of fibrillatory wave complexity in the human right atrium during paroxysmal and chronic atrial fibrillation. J. Cardiovasc. Electrophysiol. 16, 1071–1076.

Raviart, P.A., Thomas, J.M., 1977. A Mixed Finite Element Method for 2-nd Order Elliptic Problems. Springer Berlin Heidelberg, pp. 292–315.

Ronan, W., McMeeking, R.M., Chen, C.S., McGarry, J.P., Deshpande, V.S., 2015. Cooperative contractility: the role of stress fibres in the regulation of cell-cell junctions. J. Biomech. 48, 520–528.

Rossi, S., Lassila, T., Ruiz-Baier, R., Sequeira, A., Quarteroni, A., 2014. Thermodynamically consistent orthotropic activation model capturing ventricular systolic wall thickening in cardiac electromechanics. Eur. J. Mech. 48, 129–142.

Ruiz-Baier, R., 2015. Primal-mixed formulations for reaction-diffusion systems on deforming domains. J. Comput. Phys. 299, 320–338.

Sahli Costabal, F., Concha, F.A., Hurtado, D.E., Kuhl, E., 2017. The importance of mechano-electrical feedback and inertia in cardiac electromechanics. Comput. Methods Appl. Mech. Eng. 320, 352–368.

Salamhe, A., Dhein, S., 2013. Effects of mechanical forces and stretch on intercellular gap junction coupling. Biochimica et Biophysica Acta (BBA) - Biomembranes 1828 (1), 147–156.

Showalter, R., 1979. Degenerate parabolic initial-boundary value problems. J. Differ. Equ. 31 (3), 296–312.

Spencer, A.J.M., 1989. Continuum Mechanics. Longman Group Ltd, London.

Tadmor, E.B., Miller, R.E., Elliot, R.S., 2012. Continuum Mechanics and Thermodynamics: From Fundamental Concepts to Governing Equations. Cambridge University Press.

Thomas, S.P., Kucera, J.P., Bircher-Lehmann, L., Rudy, Y., Saffitz, J.E., Kléber, A.G., 2003. Impulse propagation in synthetic strands of neonatal cardiac myocytes with genetically reduced levels of connexin 43. Circ. Res. 92 (11), 1209–1216.

Tran, D.X., Sato, D., Yochelis, A., Weiss, J.N., Garfinkel, A., Qu, Z., 2009. Bifurcation and chaos in a model of cardiac early afterdepolarizations. Phys. Rev. Lett. 102, 258103.

Trayanova, N.A., Costantino, J., Gurev, V., 2011. Electromechanical models of the ventricles. Am. J. Physiol. Heart Circ. Physiol. 301, H279–H286.

Wang, W., Suo, Z., 1997. Shape change of a pore in a stressed solid via surface diffusion motivated by surface and elastic energy variation. J. Mech. Phys. Solids 45, 709–729.

Ward, M.-L., Williams, I.A., Chu, I., Cooper, P.J., Ju, Y.K., Allen, D.G., 2008. Stretch-activated channels in the heart: contributions to length-dependence and to cardiomyopathy. Prog. Biophys. Mol. Biol. 97, 232–249.

Weitsman, Y., 1987. Stress assisted diffusion in elastic and viscoelastic materials. J. Mech. Phys. Solids 35, 73–93.

Whiteley, J.P., Bishop, M.J., Gavaghan, D.J., 2007. Soft tissue modelling of cardiac fibres for use in coupled mechano-electric simulations. Bull. Math. Biol. 69, 2199–2225.

Yamazaki, M., Vaquero, L.M., Hou, L., Campbell, K., Zlochiver, S., Klos, M., Mironov, S., Berenfeld, O., Honjo, H., Kodama, I., Jalife, J., Kalifa, J., 2009. Mechanisms of stretch induced atrial fibrillation in the presence and the absence of adreno–cholinergic stimulation: interplay between rotors and focal discharges. Heart Rhythm. 6, 1009–1017.

Yuan, T.Y., Jackson, A.R., Huang, C.Y., Gu, W.Y., 2009. Strain-dependent oxygen diffusivity in bovine annulus fibrosus. J. Biomech. Eng. 131, 074503.

Zheng, Y.T., Xuan, F.Z., Wang, Z., 2015. A dominant role of stress-dependent oxide structure on diffusion flux in the strain-reaction engineering. Chem. Phys. Lett. 626, 25–28.